Improved Direct Torque Control of Induction Motor in MATLAB

Murugan R, Aasheesh Raizada, Preeti Naval and Kuldeep Singh Kulhar

Murugan R, Associate Professor, Department of Computer Science and Information Technology, Jain (Deemed to be University), Bangalore, India, Email Id-murugan@jainuniversity.ac.in
Aasheesh Raizada, Assistant Professor, Department of Computer Science Engineering, Sanskriti University, Mathura, Uttar Pradesh, India, Email Id-aasheesh.cse@sanskriti.edu.in
Preeti Naval, Assistant Professor, Maharishi School of Engineering & Technology, Maharishi University of Information Technology, Uttar Pradesh, India, Email Id-er.preetinaval09@gmail.com
Kuldeep Singh Kulhar, Professor, Civil Engineering, Vivekananda Global University, Jaipur, India, Email Id-k.singh@vgu.ac.in

Abstract: Induction motors based electric drives are dominated in many applications due to their superior characteristics over other drives including cost. An effect control method is required to reduce ripples in the torque. A direct torque control (DTC) is implemented by various scholars recently, however for further reduction of ripples in torque a modified DTC is implemented in this paper. The proposed method considerably alleviates the computational burden of control technique on chip. The selection of inverter switching vectors is identified for restricting the torque and flux errors within their respective hysteresis bands. Fastest responses of torque, speed and flux are achieved. This paper also includes the incorporation of modeling and designing of DTC with induction motor to enhance comprehension. Extensive results under various operating conditions are presented in this paper to enhance the importance of the improved DTC.

Keywords: DTC, Induction motor, SVPWM, torque ripple minimization, modeling.

Corresponding Author: murugan@jainuniversity.ac.in

1. Introduction

The history of an electrical motor is started as early as 19^{th} century. Alternating Current (AC) motors are using for various applications in many industries as well as domestic applications due to high robustness, low price, reliability, high efficiency etc. However, variable operating speed is required to do many tasks especially where used induction motors. Operating an electric drive at a low speed is commonly used for many places in industries. Among many existing speed control techniques, a direct torque control (DTC) method is exhibits superior characteristics over other methods [1-2]. Recently advanced induction motor drives with PWM inverter based novel control strategies are developed with the help of Space Vector Modulation (SVM), where the motor will be controlled independently and directly without using transformations.

Because of no direct connection among stationary and rotating parts of the motor, an induction motor is having some features over other. This implies, absence of mechanical parts such are brushes, commentators. Hence, the maintenance and size can be reduced in induction motors. Anyhow, in a variable speed drives, more mechanical energy is required. Three-phase induction motors are commonly utilized across various applications because of their ability to produce high torque. Hence a three phase inverter is required (either current source or voltage source) to regulate the speed of the motor. By managing star to delta connection, the motor were controlled before inventions of modern power electronics. However, this gives very limited speed changes. Some of efficient controls methods are listed below gather from recent publications.

- Scalar control techniques: these controllers are implemented based on constant ratio between “Voltage-Frequency” (V/f) and it is very simple method. However, this control technique unable to perform accuracy during all conditions.
- Vector control techniques: both torque and flux are controlling in these methods independently. Hence, induction motor can be able to operate as similar to separately excited DC motor. Park and Clark transformations are using to achieve this method.
- Field Acceleration method: The phase and amplitude of the stator current will be maintained constant in this approach.

The advanced approach of the vector control is a DTC approach. The DTC method is an advanced approach of the conventional vector control. The flux and torque are controlled directly through an inverter. Various features of DTC are listed below.

- Both torque and flux will be regulated directly.
- Voltages and currents of stator in a motor are regulating indirectly and they are approximately sinusoidal in nature.
- Even at stand still, it have high dynamic performance.
- Absence of co-ordinate transforms.
- The response time for torque is very less as compared with other vector control methods.

However, inherent torque ripples will be existed in a conventional DTC. Hence, a modified DTC is implemented in this paper. In Section-II, the organization of this paper entails the modeling of the induction motor and DTC. Dynamic state space model is provided in Section-III. The enhanced DTC of an induction motor is provided in Section-IV. MATLAB Simulink based results are listed in Section-V. The paper concludes with a list of references at the end.

2. Modelling of Induction Motor and DTC

Input voltage of induction motor is expressed as flowing equations to achieve the proper transformations.

$$\begin{bmatrix} V_{as} \\ V_{bs} \\ V_{cs} \end{bmatrix} = \begin{bmatrix} \cos\theta & \sin\theta & 1 \\ \cos(\theta-120^0) & \sin(\theta-120^0) & 1 \\ \cos(\theta+120^0) & \sin(\theta+120^0) & 1 \end{bmatrix} \begin{bmatrix} V_{qs}^s \\ V_{ds}^s \\ V_{os}^s \end{bmatrix} \quad (1)$$

$$\begin{bmatrix} V_{qs}^s \\ V_{ds}^s \\ V_{os}^s \end{bmatrix} = \frac{2}{3} \begin{bmatrix} \cos\theta & \cos(\theta-120^0) & \cos(\theta+120^0) \\ \sin\theta & \sin(\theta-120^0) & \sin(\theta+120^0) \\ 0.5 & 0.5 & 0.5 \end{bmatrix} \begin{bmatrix} V_{as} \\ V_{bs} \\ V_{cs} \end{bmatrix} \quad (2)$$

$$V_{as} = V_{qs}^s. \quad (3)$$

$$V_{bs} = -\frac{1}{2}V_{qs}^s - \frac{\sqrt{3}}{2}V_{ds}^s. \quad (4)$$

$$V_{cs} = -\frac{1}{2}V_{qs}^s + \frac{\sqrt{3}}{2}V_{ds}^s. \quad (5)$$

$$V_{ds}^s = -\frac{1}{\sqrt{3}}V_{bs} + \frac{1}{\sqrt{3}}V_{cs}. \quad (6)$$

$$V_{qs}^s = \frac{2}{3}V_{as} - \frac{1}{3}V_{bs} - \frac{1}{3}V_{cs} = V_{as}. \quad (7)$$

The angle $\theta_e = \omega_e t.$

$$V_{ds} = V_{qs}^s \sin\theta_e + V_{ds}^s \cos\theta_e. \quad (8)$$

$$V_{qs} = V_{qs}^s \cos\theta_e - V_{ds}^s \sin\theta_e. \quad (9)$$

$$V_{ds}^s = -V_{qs} \sin\theta_e + V_{ds} \cos\theta_e. \quad (10)$$

$$V_{qs}^s = V_{qs} \cos\theta_e + V_{ds} \sin\theta_e. \quad (11)$$

$$V_{as} = V_m \cos(\omega_e t + \phi). \quad (12)$$

$$V_{bs} = V_m \cos(\omega_e t - \frac{2\pi}{3} + \phi). \quad (13)$$

$$V_{cs} = V_m \cos(\omega_e t + \frac{2\pi}{3} + \phi). \quad (14)$$

$$V_{qs}^s = V_m \cos(\omega_e t + \phi). \quad (15)$$

$$V_{ds}^s = -V_m \sin(\omega_e t + \phi). \quad (16)$$

$$V_{qs} = \cos\phi . V_m. \quad (17)$$

$$V_{ds} = -V_m \sin\phi. \quad (18)$$

From above expressions, it shows that V_{qs}^{s} and V_{ds}^{s} are two phase balanced components.

$$\begin{aligned} \overline{V} &= V_{qds}^{s} = V_{qs}^{s} - jV_{ds}^{s} \\ &= V_{m}\left[\cos(\omega_{e}t+\phi) + j\sin(\omega_{e}t+\phi)\right] \\ &= \hat{V}_{m}e^{j\phi_{e}j\omega_{e}t} \\ &= \sqrt{2}V_{s}e^{j(\theta_{e}+\phi)} \end{aligned} \tag{19}$$

$$\overline{V} = V_{qs}^{s} - jV_{ds}^{s} = (V_{qs} - jV_{ds})e^{+j\theta_{e}}. \tag{20}$$

$$\left|\overline{V}\right| = \hat{V}_{m} = \sqrt{V_{qs}^{2} + V_{ds}^{2}}\ . \tag{21}$$

$$\begin{aligned} \overline{V} &= V_{qs}^{s} - jV_{ds}^{s} \\ &= \left(\frac{2}{3}V_{as} - \frac{1}{3}V_{bs} - \frac{1}{3}V_{cs}\right) - j\left(-\frac{1}{\sqrt{3}}V_{bs} + \frac{1}{\sqrt{3}}V_{cs}\right) \\ &= \frac{2}{3}\left[V_{as} + aV_{bs} + a^{2}V_{cs}\right] \end{aligned} \tag{22}$$

Where $a=e^{j2\Pi/3}$ and $a^2 = e^{-j2\Pi/3}$. Similar transformations of rotor wind also can be made based on above equations. For induction motor in rotating two phase synchronous frame, the following d^s -q^s and $d^r - q^r$ expressions can be attempted:

$$V_{qs}^{s} = R_{s}I_{qs}^{s} + \frac{d}{dt}\psi_{qs}^{s}. \tag{23}$$

$$V_{ds}^{s} = R_{s}I_{ds}^{s} + \frac{d}{dt}\psi_{ds}^{s}. \tag{24}$$

Similarly the other expressions which are needed in modeling of machine as well as DTC are expressed below:

$$V_{ds} = R_{s}I_{ds} + \frac{d}{dt}\psi_{ds} - \omega_{e}\psi_{qs}. \tag{25}$$

$$V_{qs} = R_{s}I_{qs} + \frac{d}{dt}\psi_{qs} + \omega_{e}\psi_{ds}. \tag{26}$$

Under non-rotating conditions, i.e., $\omega_r = 0$, the rotor expressions can be re writing as:

$$V_{dr} = \frac{d}{dt}\psi_{dr} + R_{r}i_{dr} + -\omega_{e}\psi_{qr}. \tag{27}$$

$$V_{qr} = R_{r}i_{qr} + \frac{d}{dt}\psi_{qr} + \omega_{e}\psi_{dr}. \tag{28}$$

The rotor equations will be modified as listed below in case of considering the motor speed.

$$V_{qr} = R_{r}i_{qr} + \frac{d}{dt}\psi_{qr} + (\omega_{e} - \omega_{r})\psi_{dr}. \tag{29}$$

$$V_{dr} = R_{r}i_{dr} + \frac{d}{dt}\psi_{dr} - (\omega_{e} - \omega_{r)}\psi_{qr}. \tag{30}$$

In similar way:

$$\psi_{qs} = L_{ls} i_{qs} + L_m (i_{qs} + i_{qr}). \tag{31}$$

$$\psi_{qr} = L_{lr} i_{qr} + L_m (i_{qs} + i_{qr}). \tag{32}$$

$$\psi_{qm} = L_m (i_{qs} + i_{qr}). \tag{33}$$

$$\psi_{ds} = L_m (i_{ds} + i_{dr}) + L_{ls} i_{ds}. \tag{34}$$

$$\psi_{dr} = L_m (i_{ds} + i_{dr}) + L_{lr} i_{dr}. \tag{35}$$

$$\psi_{dm} = (i_{ds} + i_{dr}) L_m .. \tag{36}$$

$$\begin{bmatrix} V_{qs} \\ V_{ds} \\ V_{qr} \\ V_{dr} \end{bmatrix} = \begin{bmatrix} R_s + SL_s & \omega_e L_s & SL_m & \omega_e L_m \\ -\omega_e L_s & R_s + SL_s & -\omega_e L_m & SL_m \\ SL_m & (\omega_e - \omega_r) L_m & R_r + SL_r & (\omega_e - \omega_r) L_r \\ -(\omega_e - \omega_r) L_m & SL_m & -(\omega_e - \omega_r) L_r & R_r + SL_r \end{bmatrix} \begin{bmatrix} i_{qs} \\ i_{ds} \\ i_{qr} \\ i_{dr} \end{bmatrix} \tag{37}$$

$$T_e = T_L + J \frac{d\omega_m}{dt} = T_L + \frac{2}{P} J \frac{d\omega_r}{dt}. \tag{38}$$

Where T_L and Te are torques of load and motor respectively, J represents motor inertia.

$$V_{qs} - jV_{ds} = R_s (i_{qs} - j i_{ds}) + \frac{d}{dt} (\psi_{qs} - j\psi_{ds}) + j\omega_e (\psi_{qs} - j\psi_{ds}). \tag{39}$$

$$V_{qdr} = R_r i_{qdr} + \frac{d}{dt} \psi_{qdr} + j(\omega_e - \omega_r) \psi_{qdr}. \tag{41}$$

$$V_{qds} = R_s i_{qds} + \frac{d}{dt} \psi_{qds} + j(\omega_e - \omega_r) \psi_{qds}. \tag{40}$$

$$V_s = R_s I_s + j\omega_e \psi_s. \tag{42}$$

$$0 = \frac{R_r}{S} I_r + j\omega_e \psi_r. \tag{43}$$

$$T_e = \frac{3}{2} \left(\frac{P}{2} \right) \overline{\psi}_m \bar{I}_r \sin \delta. \tag{44}$$

$$T_e = \frac{3}{2} \left(\frac{P}{2} \right) \overline{\psi}_m x \bar{I}_r. \tag{45}$$

$$T_e = \frac{3}{2} \left(\frac{P}{2} \right) \psi_{dm} i_{qr} - \psi_{qm} I_{dr}. \tag{46}$$

$$T_e = \frac{3}{2} \left(\frac{P}{2} \right) \psi_{dm} i_{qs} - \psi_{qm} I_{ds}. \tag{47}$$

$$T_e = \frac{3}{2} \left(\frac{P}{2} \right) \psi_{ds} i_{qs} - \psi_{qs} I_{ds}.. \tag{48}$$

$$T_e = \frac{3}{2} \left(\frac{P}{2} \right) L_m (i_{qs} i_{dr} - i_{ds} i_{qr}). \tag{49}$$

$$T_e = \frac{3}{2}\left(\frac{P}{2}\right)(\psi_{dr} i_{qr} - \psi_{qr} I_{dr}) . \tag{50}$$

However,

$$V_{qs}^s = R_s i_{qs}^s + \frac{d}{dt}\psi_{qs}^s . \tag{51}$$

$$V_{ds}^s = R_s i_{ds}^s + \frac{d}{dt}\psi_{ds}^s . \tag{52}$$

$$0 = R_r i_{qr}^s + \frac{d}{dt}\psi_{qr}^s - \omega_r \psi_{dr}^s . \tag{53}$$

$$0 = R_r i_{dr}^s + \frac{d}{dt}\psi_{dr}^s + \omega_r \psi_{qr}^s . \tag{54}$$

$$T_e = \frac{3}{2}\left(\frac{P}{2}\right)\psi_{dm}^s i_{qr}^s - \psi_{qm}^s i_{dr}^s . \tag{55}$$

$$T_e = \frac{3}{2}\left(\frac{P}{2}\right)\psi_{dm}^s i_{qs}^s - \psi_{qm}^s i_{ds}^s . \tag{56}$$

$$T_e = \frac{3}{2}\left(\frac{P}{2}\right)\psi_{ds}^s i_{qs}^s - \psi_{qs}^s i_{ds}^s . \tag{57}$$

$$T_e = \frac{3}{2}\left(\frac{P}{2}\right)L_m (i_{ds}^s i_{dr}^s - i_{ds}^s i_{qr}^s) . \tag{58}$$

$$T_e = \frac{3}{2}\left(\frac{P}{2}\right)(\psi_{dr}^s i_{qr}^s - \psi_{qr}^s i_{dr}^s) . \tag{59}$$

$$V_{qds}^s = R_s i_{qds}^s + \frac{d}{dt}\psi_{qds}^s . \tag{60}$$

$$0 = R_r i_{qds}^s + \frac{d}{dt}\psi_{qdr}^s - j\omega_r \psi_{qdr}^s . \tag{61}$$

3. State Space Model

In order to analyze the transient responses of the motor, the state space analysis should be done.

$$F_{ds} = \omega_b \psi_{ds} . \tag{62}$$

$$F_{dr} = \omega_b \psi_{dr} . \tag{63}$$

$$F_{qs} = \omega_b \psi_{qs} . \tag{64}$$

$$F_{qr} = \omega_b \psi_{qr} . \tag{65}$$

$$v_{qs} = R_s i_{qs} + \frac{1}{\omega_b}\frac{dF_{qs}}{dt} + \frac{\omega_e}{\omega_b} F_{ds} . \tag{66}$$

$$v_{ds} = R_s i_{ds} + \frac{1}{\omega_b}\frac{dF_{ds}}{dt} + \frac{\omega_e}{\omega_b}F_{qs}. \tag{67}$$

$$0 = R_r i_{qr} + \frac{1}{\omega_b}\frac{dF_{qr}}{dt} + \frac{(\omega_e - \omega_r)}{\omega_b}F_{dr}. \tag{68}$$

$$0 = R_r i_{dr} + \frac{1}{\omega_b}\frac{dF_{dr}}{dt} + \frac{(\omega_e - \omega_r)}{\omega_b}F_{qr}. \tag{69}$$

$$F_{qs} = \omega_b \psi_{qs} = X_{ls} i_{qs} + X_m (i_{qs} + i_{qr}). \tag{70}$$

$$Fr = \omega_b \psi r = X_{lr} i_{qr} + X_m (i_{qs} + i_{qr}). \tag{71}$$

$$F_{qm} = \omega_b \psi_{qm} = X_m (i_{qs} + i_{qr}). \tag{72}$$

$$F_{ds} = \omega_b \psi_{ds} = X_{ls} i_{ds} + X_m (i_{ds} + i_{dr}). \tag{73}$$

$$F_{dr} = \omega_b \psi_{dr} = X_{lr} i_{dr} + X_m (i_{ds} + i_{dr}). \tag{74}$$

$$F_{dm} = \omega_b \psi_{dm} = X_m (i_{ds} + i_{dr}). \tag{75}$$

Where $X_{ls} = \omega_b L_{ls}$, $X_{lr} = \omega_b L_{lr}$, and $X_m = \omega_b L_m$, or

$$F_{qs} = X_{ls} i_{qs} + F_{qm}. \tag{76}$$

$$F_{qr} = X_{lr} i_{qr} + F_{qm}. \tag{77}$$

$$F_{ds} = X_{ls} i_{ds} + F_{dm}. \tag{78}$$

$$F_{dr} = X_{lr} i_{dr} + F_{dm}. \tag{79}$$

Hence, $$i_{qs} = \frac{F_{qs} - F_{qm}}{X_{ls}}. \tag{80}$$

$$i_{qr} = \frac{F_{qr} - F_{qm}}{X_{lr}}. \tag{81}$$

$$i_{ds} = \frac{F_{ds} - F_{dm}}{X_{ls}}. \tag{82}$$

$$i_{dr} = \frac{F_{dr} - F_{dm}}{X_{lr}}. \tag{83}$$

Therefore, $$F_{qm} = X_m \left[\frac{F_{qs} - F_{qm}}{X_{ls}} + \frac{F_{qr} - F_{qm}}{X_{lr}} \right]. \tag{84}$$

$$F_{qm} = X_{m1} \left[\frac{F_{qs}}{X_{ls}} + \frac{F_{qr}}{X_{lr}} \right]. \tag{85}$$

Where

$$X_{m1} = \frac{1}{\left(\frac{1}{X_m} + \frac{1}{X_{ls}} + \frac{1}{X_{lr}} \right)}.$$

$$F_{dm} = X_{m1}\left[\frac{F_{ds}}{X_{ls}} + \frac{F_{dr}}{X_{lr}}\right]. \tag{86}$$

$$v_{qs} = \frac{R_s}{X_{ls}}(F_{qs} - F_{qm}) + \frac{1}{\omega_b}\frac{dF_{qs}}{dt} + \frac{\omega_e}{\omega_b}F_{ds}. \tag{87}$$

$$v_{ds} = \frac{R_s}{X_{ls}}(F_{ds} - F_{dm}) + \frac{1}{\omega_b}\frac{dF_{ds}}{dt} - \frac{\omega_e}{\omega_b}F_{qs}. \tag{88}$$

$$0 = \frac{R_r}{X_{lr}}(F_{qr} - F_{qm}) + \frac{1}{\omega_b}\frac{dF_{qr}}{dt} + \frac{(\omega_e - \omega_r)}{\omega_b}F_{dr}. \tag{89}$$

$$0 = \frac{R_r}{X_{lr}}(F_{dr} - F_{dm}) + \frac{1}{\omega_b}\frac{dF_{dr}}{dt} + \frac{(\omega_e - \omega_r)}{\omega_b}F_{qr} \tag{90}$$

$$\frac{dF_{qs}}{dt} = \omega_b\left[v_{qs} - \frac{\omega_e}{\omega_b}F_{ds} - \frac{R_s}{X_{ls}}(F_{qs} - F_{qm})\right]. \tag{91}$$

$$\frac{dF_{ds}}{dt} = \omega_b\left[v_{ds} + \frac{\omega_e}{\omega_b}F_{qs} - \frac{R_s}{X_{ls}}(F_{ds} - F_{dm})\right]. \tag{92}$$

$$\frac{dF_{qr}}{dt} = -\omega_b\left[\frac{(\omega_e - \omega_r)}{\omega_b}F_{dr} + \frac{R_r}{X_{lr}}(F_{qr} - F_{qm})\right]. \tag{93}$$

$$\frac{dF_{dr}}{dt} = -\omega_b\left[-\frac{(\omega_e - \omega_r)}{\omega_b}F_{qr} + \frac{R_r}{X_{lr}}(F_{dr} - F_{dm})\right] \tag{94}$$

$$T_e = \frac{3}{2}\left(\frac{P}{2}\right)\frac{1}{\omega_b}(F_{ds}i_{qs} - F_{qs}i_{ds}). \tag{95}$$

4. Improved DTC

In a conventional DTC, more ripples will be existed in the electromagnetic torque. Optimal sector for switching pulses are obtained from below basic equations.

$$\bar{T}_e = \frac{3}{2}\left(\frac{P}{2}\right)\bar{\psi}_s\,\bar{I}_s \tag{96}$$

$$\bar{\psi}_s = L_s\bar{I}_s + L_m\bar{I}_r \tag{97}$$

$$\bar{\psi}_r = L_m\bar{I}_s + L_r\bar{I}_r. \tag{98}$$

$$\bar{\psi}_s = \frac{L_m}{L_r}\bar{\psi}_r + L_s^{'}\bar{I}_s \tag{99}$$

$$\bar{I}_s = \frac{1}{L_s^{'}}\bar{\psi}_s - \frac{L_m}{L_r L_s^{'}}\bar{\psi}_r \tag{100}$$

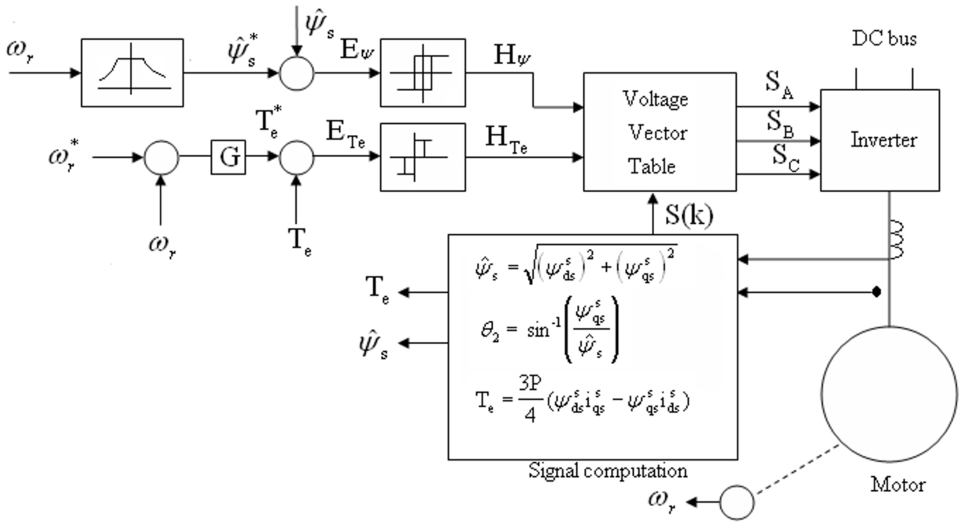

Fig. 1: Improved DTC of Induction motor.

$$\overline{T}_e = \frac{3}{2}\left(\frac{P}{2}\right)\frac{L_m}{L_r L_s^{'}}\overline{\psi}_r \overline{\psi}_s \tag{101}$$

That is, the magnitude torque is

$$\overline{T}_e = \frac{3}{2}\left(\frac{P}{2}\right)\frac{L_m}{L_r L_s^{'}}\left|\overline{\psi}_r\right|\left|\overline{\psi}_s\right|\sin\gamma \tag{102}$$

Incremental of $\Delta\gamma$, the torque $\Delta\overline{T}_e$ expression is given as

$$\Delta\overline{T}_e = \frac{3}{2}\left(\frac{P}{2}\right)\frac{L_m}{L_r L_s^{'}}\left|\overline{\psi}_r\right|\left|\overline{\psi}_s + \Delta\overline{\psi}_s\right|\sin\Delta\gamma \tag{103}$$

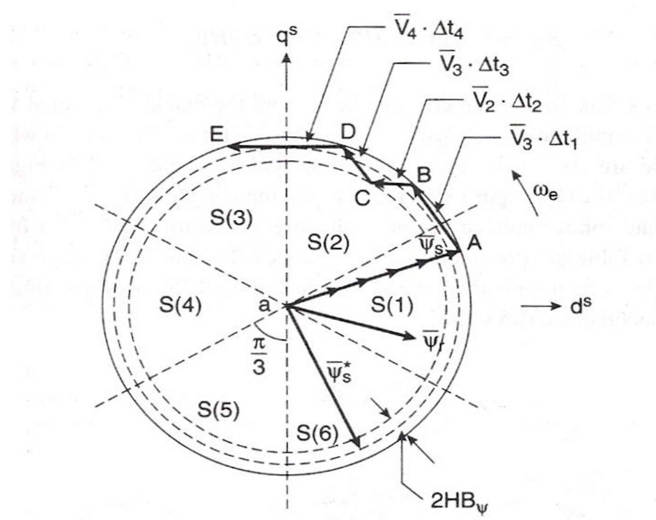

Fig. 2: Space Vector Strategy.

The block diagram of improved direct flux and torque controller is depicted in Fig. 1.

$$H_{\psi} = 1 \quad \text{for} \quad E_{\psi} > +HB_{\psi} \tag{104}$$

$$H_{\psi} = -1 \quad \text{for} \quad E_{\psi} < -HB_{\psi} \tag{105}$$

$$H_{Te} = 1 \quad \text{for} \quad E_{Te} > +HB_{Te} \tag{106}$$

$$H_{Te} = -1 \quad \text{for} \quad E_{Te} < -HB_{Te}. \tag{107}$$

$$H_{Te} = 0 \quad \text{for} \quad -HB_{Te} < E_{Te} < +HB_{Te}. \tag{108}$$

Motor voltages and currents are helpful to calculate the torque and flux components. Space vector strategy is applied to achieve the delivered pulse sequence as shown in Fig. 2.

The input signals H_{ψ}, H_{Te}, are used to decide the pulse sequence as per below table by using the following equations.

$$\overline{V}_s = \frac{d}{dt}(\overline{\psi}_s) \tag{109}$$

Or

$$\Delta \overline{\psi}_s = \overline{V}_s \,.\Delta t \tag{110}$$

Table1: SVM vectors selection.

V	V_1.	V_2.	V_3.	V_4.	V_5.	V_6.	$V_{0,7}$
Ψ_s	↑	↑	↓	↓	↓	↑	0
T_e	↓	↑	↑	↑	↓	↓	↓

5. Improved DTC

A model using MATLAB/Simulink has been developed to showcase the findings. Various models are modeled in Simulink components and used to construct the improved DTC as shown in Fig. 3.

Reponses under considering of changes in torque and speed are carryout in this section. Following results are obtained and which are having satisfactory responses during both steady state and transient period. Corresponding stator flux is given in Fig. 4. A stable flux is achieved by proposed method. Voltage of stator phase –A is depicted in Fig. 5. Load torque and electromagnetic torques are overlapped in Fig. 6. The motor electromagnetic torque generated by motor with help of proposed DTC can be observed from Fig. 6. Flux trajectory of motor is given in Fig. 7. Various speed references and motor speed including negative speeds are listed in Fig. 8 and Fig. 9. Corresponding stator flux and currents are shown in Fig. 10 and Fig. 11.

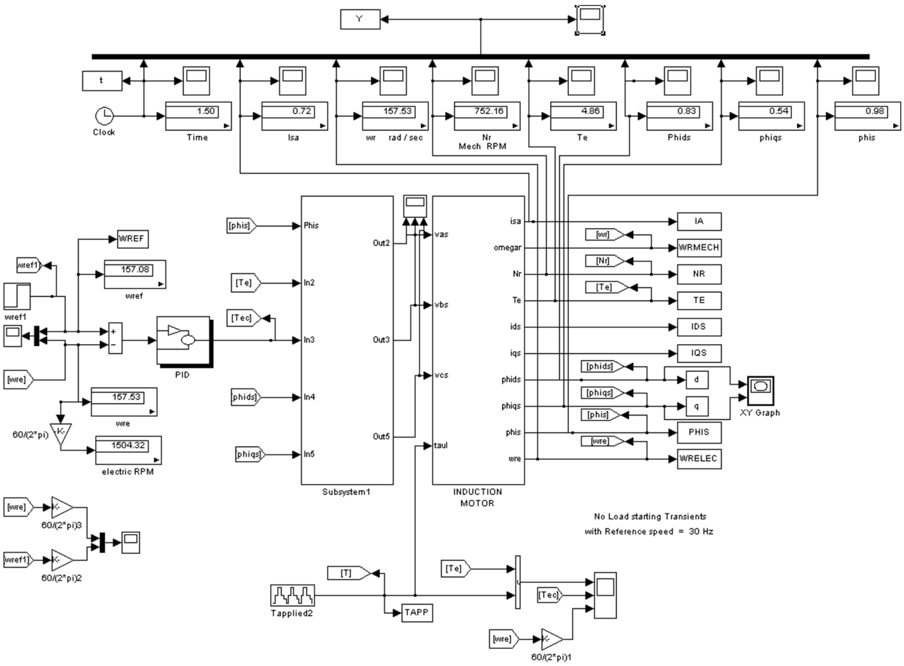

Fig. 3: Simulink model of improved DTC of induction motor.

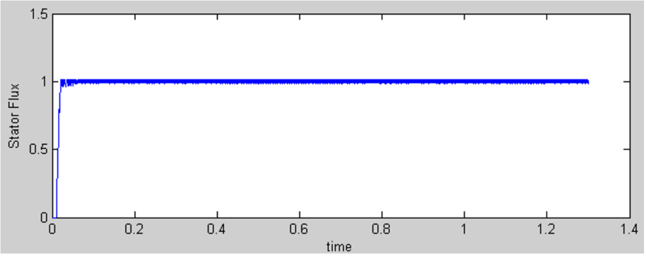

Fig. 4: Stator flux.

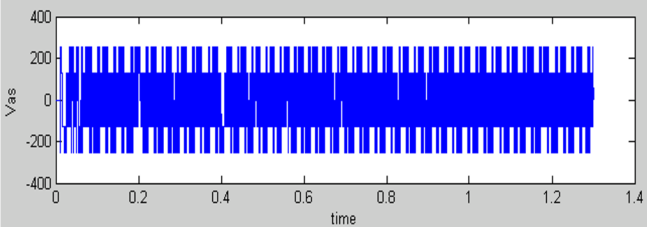

Fig. 5: Vas

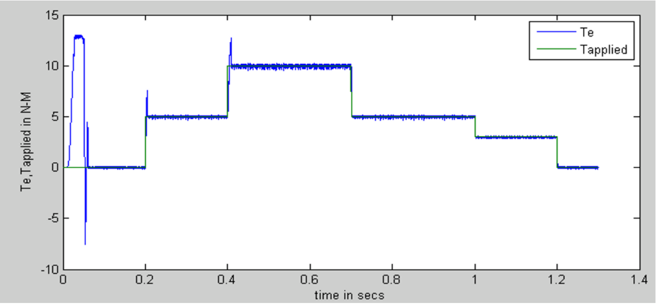

Fig. 6: T_l and Te.

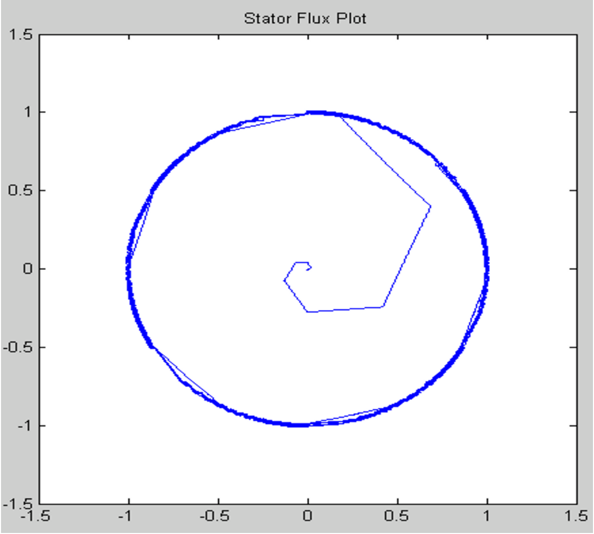

Fig. 7: Hexagonal Flux plot.

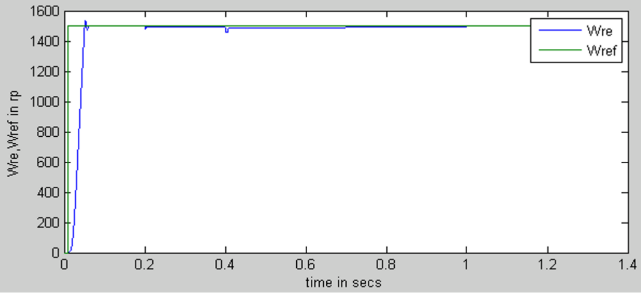

Fig. 8: speed in rpm.

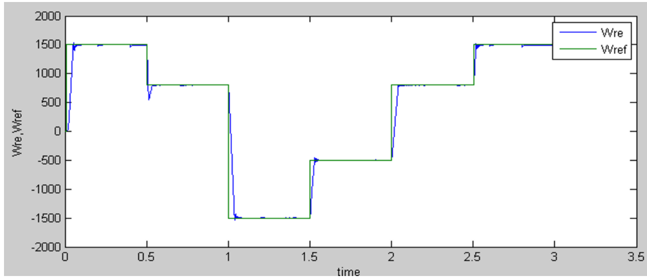

Fig. 9: Speed changes.

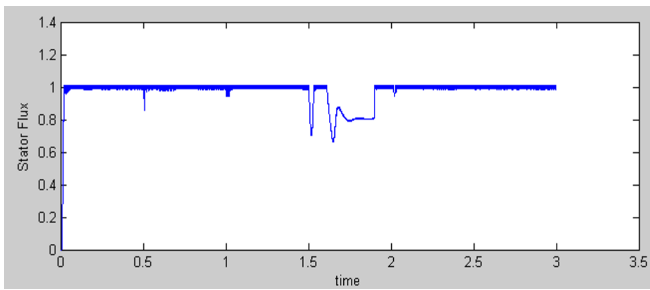

Fig. 10: Stator Flux.

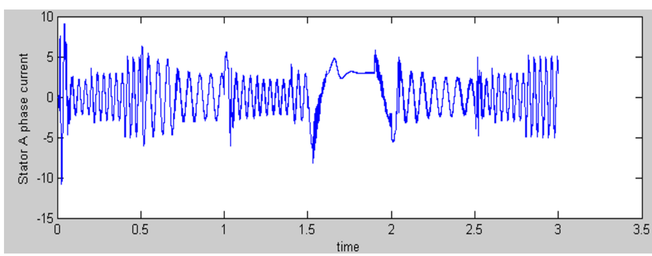

Fig. 11: Stator current – phase A.

6. Conclusions

This paper presents an enhanced direct torque control technique for induction motors. Detailed modeling of both induction motor and DTC are provided in this paper. In order to select a proper vector sequences are also listed in this paper which is made to restrict the errors of torque and flux within the respective torque and flux hysteresis bands. The proposed method is made to achieve fast responses of torque, flux and speed under sudden variations. The MATLAB/SIMULINK platform is utilized to observe the performance of direct torque control in induction motors.

References:

[1]. S. G. Malla, "A review on Direct Torque Control (DTC) of induction motor: With applications of fuzzy," 2016 International Conference on Electrical, Electronics, and Optimization Techniques (ICEEOT), Chennai, India, 2016, pp. 4557-4567, doi: 10.1109/ICEEOT.2016.7755579.

[2]. S. G. Malla, M. H. L. Rao, J. M. R. Malla, R. R. Sabat, J. Dadi and M. M. Das, "SVM-DTC Permanent magnet synchronous motor driven electric vehicle with bidirectional converter," 2013 International Mutli-Conference on Automation, Computing, Communication, Control and Compressed Sensing (iMac4s), Kottayam, India, 2013, pp. 742-747, doi: 10.1109/iMac4s.2013.6526505.

[3]. Priyanka Malla, “TSK Fuzzy Controller for Vector Control of Induction Motor”, International Journal of New Technologies in Science and Engineering (IJNTSE), Vol. 8, Issue. 1, pp. 8-12, Jan. 2022.
[4]. Siva Ganesh Malla, “Modeling of 5-Phase Induction Motor: A Review”, International Journal of New Technologies in Science and Engineering (IJNTSE), Vol. 8, Issue. 3, pp. 1-8, March. 2022.
[5]. L. Dube and E. Bayoumi, "Robust DTC Against Parameter Variation for Three Phase Induction Motor Drive Systems," 2020 International Conference on Electrical, Communication, and Computer Engineering (ICECCE), Istanbul, Turkey, 2020, pp. 1-6, doi: 10.1109/ICECCE49384.2020.9179205.
[6]. H. Sudheer, S. K. Fodad and B. Sarvesh, "Implementaion of SVM-DTC of induction motor using FPGA," 2017 IEEE International Conference on Power, Control, Signals and Instrumentation Engineering (ICPCSI), Chennai, India, 2017, pp. 2319-2323, doi: 10.1109/ICPCSI.2017.8392131.
[7]. J. Listwan and K. Pienkowski, "Experimental Studies of DTC-SVM Control of Six-Phase Induction Motor with Application of the Super-Twisting Sliding Mode Controllers," 2018 International Symposium on Electrical Machines (SME), Andrychow, Poland, 2018, pp. 1-6, doi: 10.1109/ISEM.2018.8442606.
[8]. R. Pandey, A. K. Panda and N. Patnaik, "Comparative Performance Analysis of DTC fed Three-Phase and Five-Phase Induction Motor," 2020 5th International Conference on Devices, Circuits and Systems (ICDCS), Coimbatore, India, 2020, pp. 162-166, doi: 10.1109/ICDCS48716.2020.243572.
[9]. B. Chikondra, U. R. Muduli and R. Kumar Behera, "Fault-Tolerant DTC Technique for Five-phase Three-Level NPC Inverter-fed Induction Motor Drive with an Open-Phase Fault," 2019 IEEE Energy Conversion Congress and Exposition (ECCE), Baltimore, MD, USA, 2019, pp. 5281-5287, doi: 10.1109/ECCE.2019.8912513.
[10]. V. S. R. C and S. Devabhaktuni, "Low speed Performance improvement of Constant Switching Frequency DTC of Five phase Induction Motor," 2021 National Power Electronics Conference (NPEC), Bhubaneswar, India, 2021, pp. 01-06, doi: 10.1109/NPEC52100.2021.9672519.
[11]. U. R. Muduli, B. Chikondra and R. K. Behera, "Space Vector PWM Based DTC Scheme With Reduced Common Mode Voltage for Five-Phase Induction Motor Drive," in IEEE Transactions on Power Electronics, vol. 37, no. 1, pp. 114-124, Jan. 2022, doi: 10.1109/TPEL.2021.3092259.
[12]. U. R. Muduli, B. Chikondra, M. J. Akhtar, O. Al Zaabi, K. Al Hosani and R. K. Behera, "Comparison of SVPWM Techniques Under Switching Loss Control for Induction Motor Drive With LC Filters," in IEEE Transactions on Industry Applications, vol. 59, no. 2, pp. 1849-1862, March-April 2023, doi: 10.1109/TIA.2022.3231841.
[13]. U. R. Muduli, R. K. Behera, K. Al Hosani and M. S. E. Moursi, "Direct Torque Control With Constant Switching Frequency for Three-to-Five Phase Direct Matrix Converter Fed Five-Phase Induction Motor Drive," in IEEE Transactions on Power Electronics, vol. 37, no. 9, pp. 11019-11033, Sept. 2022, doi: 10.1109/TPEL.2022.3167477.
[14]. U. R. Muduli, K. A. Hosani, K. A. Jaafari, J. Y. Alsawalhi, A. S. Al-Sumaiti and R. K. Behera, "ANN based On-board Fault Diagnostic for Induction Motor Drive in Low-Cost Electric Vehicles," 2022 IEEE Applied Power Electronics Conference and Exposition (APEC), Houston, TX, USA, 2022, pp. 153-158, doi: 10.1109/APEC43599.2022.9773566.
[15]. B. Chikondra, U. R. Muduli and R. K. Behera, "Improved DTC Technique for THL-NPC VSI Fed Five-Phase Induction Motor Drive Based on VVs Assessment Over a Wide Speed Range," in IEEE Transactions on Power Electronics, vol. 37, no. 2, pp. 1972-1981, Feb. 2022, doi: 10.1109/TPEL.2021.3102963.